MULTIFRAGMENTATION IN THE 1.8 - 4.8 GeV $^{3}He + ^{nat}Ag$, ^{197}Au REACTIONS

K. Kwiatkowski, K.B. Morley, E. Renshaw Foxford, D.S. Bracken,
V.E. Viola and N.R. Yoder
Indiana University and IUCF, Bloomington, Indiana 47408

C. Volant, E.C. Pollacco and R. Legrain
DAPNIA/SEPhN, CEN, Senclay, France

R.G. Korteling
Simon Fraser University, Burnaby, BC, Canada

J. Brzychczyk
Jagiellonian University, Krakow, Poland

H. Breuer
University of Maryland, College Park, Maryland 20742

W.A. Friedman
University of Wisconsin, Madison, Wisconsin 53706

When nuclei are subjected to extreme conditions of thermal or compressional energy, multifragmentation of the system occurs with high probability. The nature of this disintegration process is of great current interest in that it provides insight into the nuclear equation of state at low density. Analysis of previous data has indicated that multifragmentation occurs at relatively low densities[1-3] ($\rho/\rho_0 \sim 0.3 - 0.4$), suggesting that expansion of nuclear matter plays an important role in the breakup dynamics.

Investigation of multifragmentation with light-ion beams[1] (H and He) complements heavy-ion probes[2,3] in that only thermal excitation of the system should be important; i.e., compressional and rotational energy of the system should be minimal with light ions. In addition, the transport codes necessary for evaluation of the excitation energy distribution of the fragmenting nuclei should be most reliable for light-ion projectiles. However, because the energy dissipation covers a very broad range of residual excitations, it is imperative that these codes be well understood–an additional objective of these studies. Light ions also posess the experimental advantages of unique source definition and high sensitivity to the full spectrum of light-charged particle (LCP) and intermediate–mass fragments (IMF: $3 \leq Z \leq 15$) that characterize multifragmentation events.

In the present work, multifragmentation has been studied with the Indiana Silicon Sphere 4π detector (ISiS) using ^{3}He beams between 1.8 and 4.8 GeV from the Saturne II accelerator in Saclay, France. Targets of 1.0 mg/cm^2 ^{nat}Ag and 1.5 mg/cm^2 ^{197}Au

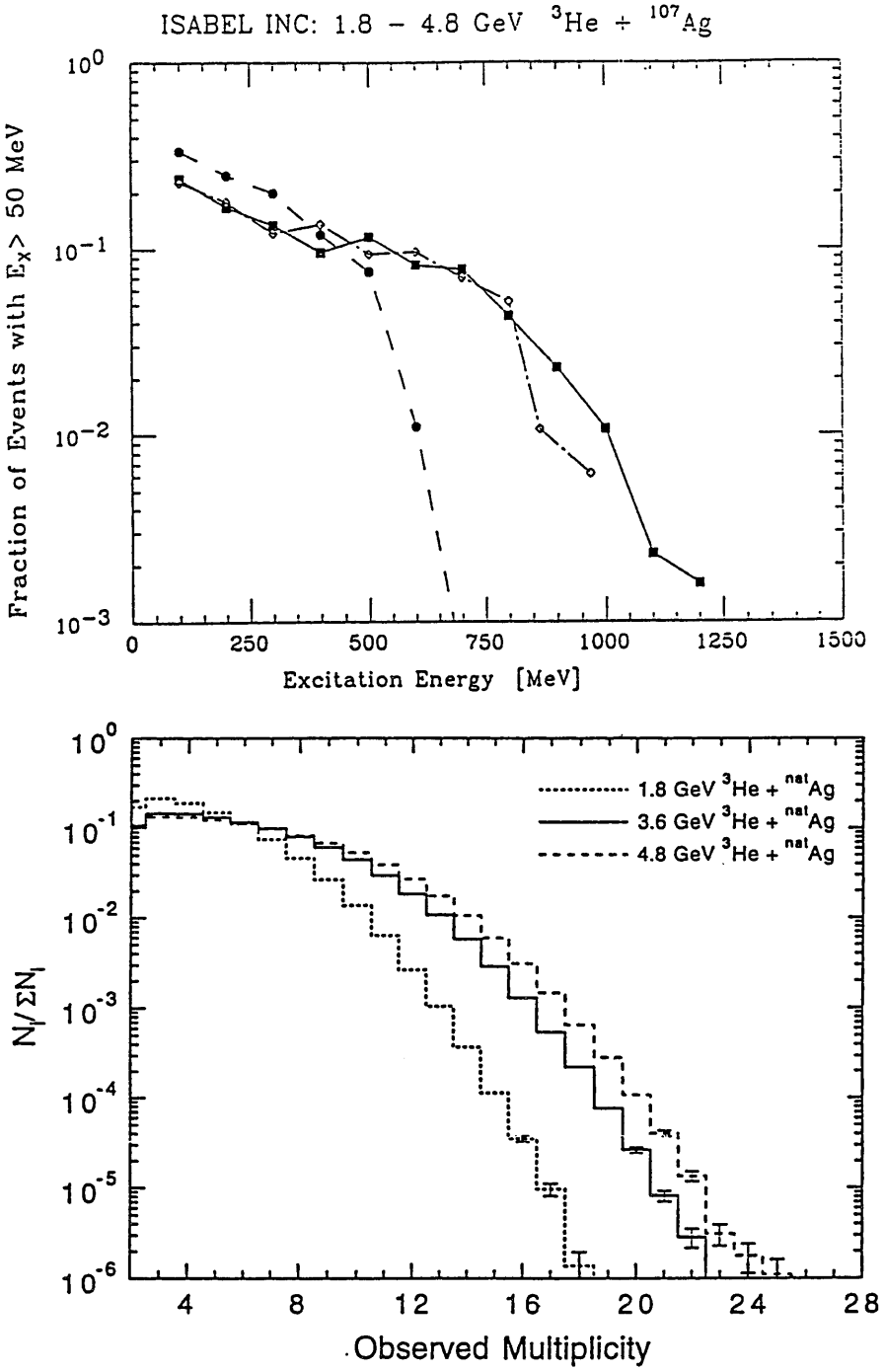

Figure 1(top): Intranuclear cascade calculations of deposition energy distributions for the same systems as shown in Fig. 1(bottom).

Figure 1(bottom): Experimental multiplicity distributions for charged particles emitted in the $^3\mathrm{He} + {}^{\mathrm{nat}}\mathrm{Ag}$ reaction at 1.8 (•), and 3.6 (◇) and 4.8 (■)GeV.

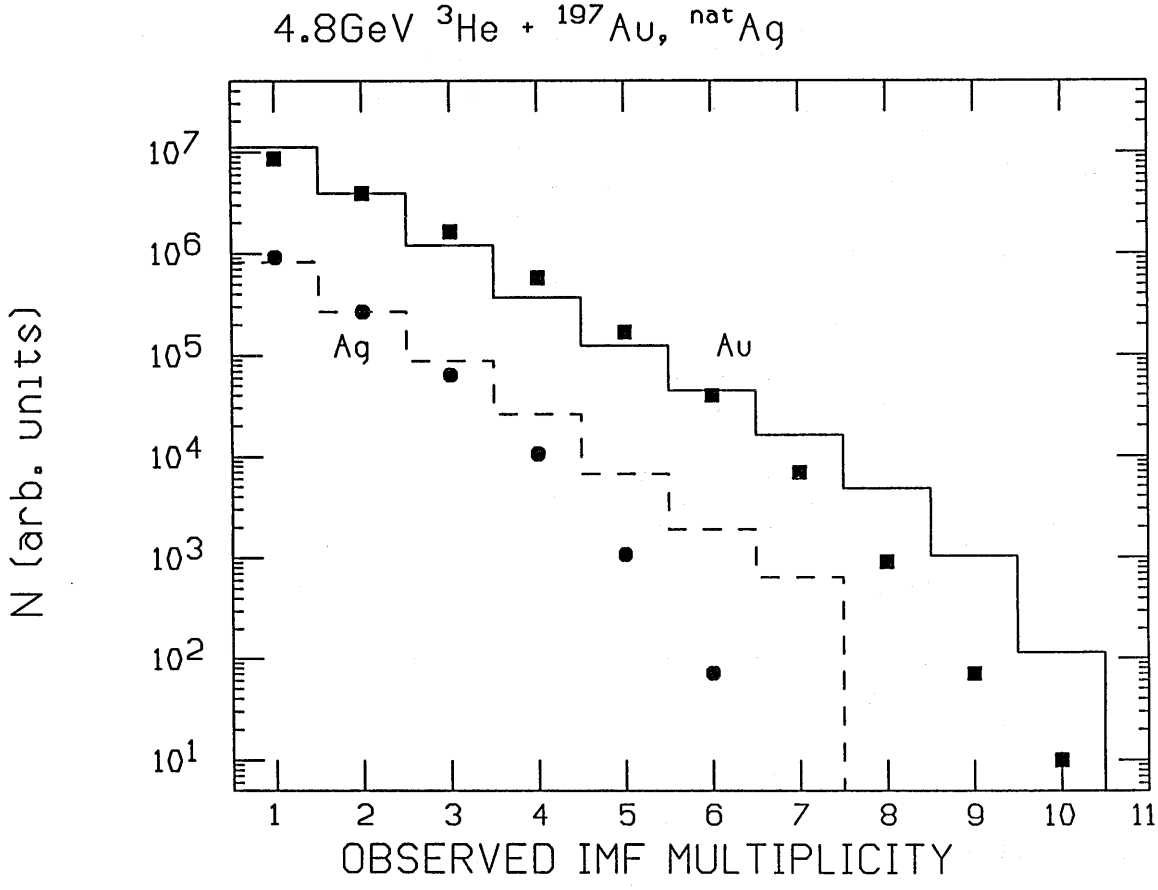

Figure 2: Multiplicity distributions for IMFs emitted from 4.8 GeV ^{3}He + ^{nat}Ag(•) and ^{197}Au (■) reactions. Histograms show predictions of the INC/EES calculation,[5] passed through the experimental detector filter.

were bombarded with ^{3}He beams with intensities approximately 5×10^{7} particles per spill. The ISiS detector, described elsewhere in this report, contains 162 low-threshold triple telescopes that permit identification of Z=1 to $\sim$ 20 fragments over a dynamic range of 0.6 MeV $\leq$ E/A $\leq$ 96 MeV. In order to trigger the data acquisition system, signals (LCP and/or IMF) were required in two or more silicon detectors.

In Fig. 1(bottom), the multiplicity distributions of charged particles are shown for three systems: ^{3}He + ^{nat}Ag at 1.8, 3.6 and 4.8 GeV. It is clear that the deposition energy increases significantly between 1.8 and 3.6 GeV. The distributions for 3.6 and 4.8 GeV ^{3}He are nearly identical, however, indicating a saturation in deposition energy in this region. In Fig. 1(top), predictions of the excitation energy distributions by the ISABEL intranuclear cascade code[4] are shown for these same systems. The qualitative agreement is apparent.

The IMF multiplicity distributions for ^{nat}Ag and ^{197}Au targets at 4.8 GeV are compared in Fig. 2. The probability for producing high multiplicity events is clearly much greater for the heavier ^{197}Au nucleus–in part due to the larger mass of the system and

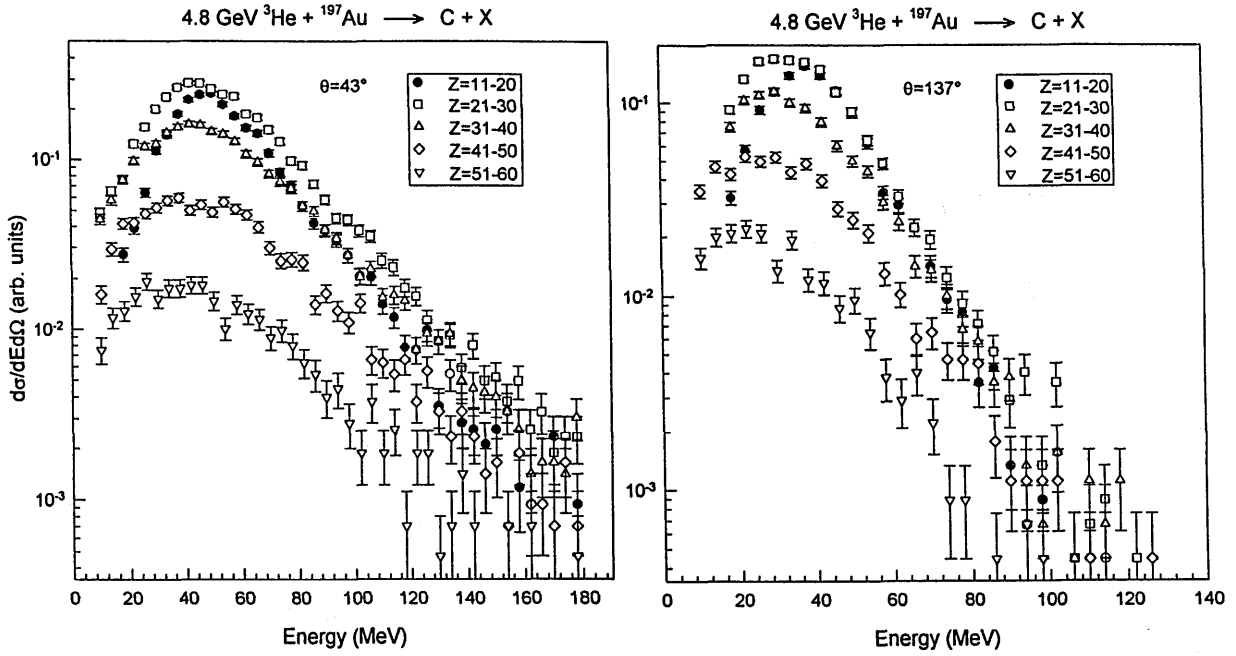

Figure 3: Kinetic energy spectra for IMFs, gated on total observed charge, $\sum Z_{obs}$. Bin size is indicated on the figure.

in part due to the high average deposition energy (although $\langle E^*/A \rangle$ is actually higher for silver). Also shown in Fig. 2 are predictions by a hybrid calculation[5] based on the ISABEL INC[4] code to predict the reaction dynamics and the expanding, evaporating source model to account for multifragmentation.[6] Freezeout of IMFs occurs near $\rho/\rho_0 \approx 0.3$ in this model. Here the model calculations have been passed through the detector geometry filter using the GEANT code.[7] For low multiplicities, the agreement is relatively good; at higher multiplicities the calculation tends to overpredict the IMF multiplicity somewhat.

The IMF multiplicities observed here, while substantial, are generally lower than observed in heavy-ion-induced reactions.[2,3] This result is in disagreement with Ref. 8, which reported larger IMF multiplicities with light ions. However, the experimental set-up for Ref. 8 involved a trigger bias (requiring at least one IMF in a few trigger detectors) and did not provide discrete charge resolution of associated fragments in its 4π array.

Several variables have been investigated as possible indicators of energy deposition, among these LCP multiplicity, Z_{bound} (total charge > 2), total observed charge ($\sum Z_{obs}$) and total transverse energy. All of these correlate, with the latter two appearing to be most sensitive. In Fig. 3 the energy spectra of carbon fragments emitted at $\langle \Theta \rangle = 43°$ and $\langle \Theta \rangle = 137°$ are shown for various cuts on $\sum Z_{obs}$ observed in the 4.8 GeV ^{3}He + ^{197}Au system. For low $\sum Z_{obs}$ these Maxwellian-like spectra exhibit a classical Coulomb peak and slope parameters of $\sim$ 5 MeV–characteristic of IMF emission at low energies. With increasing violence of the reaction (larger $\sum Z_{obs}$), the Coulomb peaks broaden systemically to lower energies and slope parameters near $\sim$ 15 MeV are reached. Beyond $\sum Z_{obs} \gtrsim 40$, the spectral shapes are approximately constant. This behavior is consistent with the expansion of the source prior to breakup, as predicted by the INC/EES calculations discussed above.

1. S.J. Yennello, *et al.*, Phys. Rev. Lett. **67**, 671 (1991); Phys. Lett. **B246**, 26 (1990).
2. R.T de Souza, *et al.*, Phys. Lett. **B268**, 6 (1991).
3. J. Hubele, *et al.*, Z. Phys. **A340**, 263 (1991); Bao-An Li, *et al.*, Phys. Lett. **308**, 225 (1993).
4. Y. Yariv and Z. Fraenkel, Phys. Rev. C **24**, 488 (1981).
5. K. Kwiatkowski, *et al.*, Phys. Rev. C **49**, 1516 (1994).
6. W.A Friedman, Phys. Rev. C **42**, 667 (1990).
7. CERN Library.
8. V. Lips, *et al.*, Phys. Rev. Lett. **72**, 1604 (1994).